Contribution from the Department of Chemistry and Laboratory for Molecular Structure and Bonding, Texas A&M University, College Station, Texas 77843, and Department of Chemistry, The University of Glasgow, Glasgow G128QQ, United Kingdom

Syntheses, Structures, and Circular Dichroism Spectra of β-$Mo_2X_4(S,S\text{-dppb})_2$ (X = Cl, Br; *S,S*-dppb = (2*S*,3*S*)-Bis(diphenylphosphino)butane)

Pradyot A. Agaskar,[1a] F. Albert Cotton,*[1a] Iain F. Fraser,[1b] Ljubica Manojlovic-Muir,[1b] Kenneth W. Muir,[1b] and Robert D. Peacock*[1b]

Received January 7, 1986

The electronic absorption spectra and circular dichroism (CD) spectra of the chiral molecules β-$Mo_2X_4(S,S\text{-dppb})_2$, with X = Cl, Br and *S,S*-dppb = (2*S*,3*S*)-bis(diphenylphosphino)butane, have been investigated and correlated with the structures of the molecules, which have been determined by X-ray crystallography. The chloro compound was obtained in two crystalline forms. For β-$Mo_2Cl_4(S,S\text{-dppb})\cdot C_4H_8O$ the crystals belong to space group $P2_12_12_1$ with a = 14.57 (1) Å, b = 36.69 (1) Å, c = 11.84 (1) Å, V = 6329 (12) Å^3, and Z = 4. For β-$Mo_2Cl_4(S,S\text{-dppb})_2\cdot 4CH_3CN$ the space group is again $P2_12_12_1$ with a = 13.535 (3) Å, b = 21.044 (7) Å, c = 23.214 (3) Å, V = 6612 (6) Å^3, and Z = 4. The molecular structures in these two crystalline forms are practically identical. The average P–Mo–Mo–P torsion angles are 24 [2] and 22 [1]° in the two cases. The bromo compound crystallizes without solvent in space group $P2_1$ with a = 16.78 (1) Å, b = 16.98 (1) Å, c = 27.19 (1) Å, β = 97.35 (3)°, V = 7685 (9) Å, and Z = 4. The two independent molecules in the unit cell have almost identical structures, with an average P–Mo–Mo–P torsion angle of 21.7 [4]°. The absorption and CD spectra of both $Mo_2X_4(S,S\text{-dppb})_2$ molecules have been recorded. In addition to three CD features that correspond to the absorption maxima, there are four others; assignments are suggested for all of them. It is shown that for the Λ absolute configuration with P–Mo–Mo–P torsion angles <45° a negative CD is expected (and observed) for the $\delta_{xy} \rightarrow \delta^*_{xy}$ transition. The weak absorptions at 470 and 490 nm (in the Cl and Br compounds, respectively) with positive CD have very large dissymmetry factors and are assigned to the $\delta_{xy} \rightarrow \delta_{x^2-y^2}$ transition. With the help of a SCF–Xα–SW calculation the remaining CD features are also assigned.

Introduction

The structures of compounds of the type β-$Mo_2X_4(PP)_2$, where X = Cl, Br and PP is a diphosphine ligand, have been the object of intense study[2-11] in the last few years. Table I is an exhaustive list of all such compounds whose crystal structures have been determined and also gives the synthetic routes that lead to them.

All these molecules have a d^4–d^4 Mo_2^{4+} moiety with two phosphorus atoms and two halogen atoms ligating each of the Mo atoms. The similar atoms are disposed trans to each other and the two *trans*-MoX_2P_2 units are rotated relative to each other about the Mo–Mo bond, so that the Mo–L bonds in one such unit do not eclipse any of the Mo–L bonds in the other. The torsion angle P–Mo–Mo–P, henceforth referred to as the ϕ angle, may have any value between 0 and 90°.

The molecules $Mo_2X_4(dppm)_2$, X = Cl, Br,[9,11] and $Mo_2Cl_4(PMe_3)_4$[12] have ϕ angles of 0 and 90°, respectively. Their principal structural parameters are listed in Tables II and III along with those of the compounds listed in Table I.

The value of the ϕ angle is determined by the balance that is struck between the steric requirements of the substituents on the phosphorus atom, which tend to make the ϕ angle deviate from 0°, and the strength of the δ bond, which is a maximum when this angle is 0 or 90°.[13]

As a result of the systematic variation of the δ overlap with the ϕ angle, the Mo–Mo bond distance and the $\delta \rightarrow \delta^*$ transition energy are correlated[2,3] with cos 2χ, where χ = 0 or $\pi/2 - \phi$ when $\phi < 45°$ or $\phi > 45°$, respectively. The closing of the δ–δ^* gap also results in a significant population of the $\delta^1\delta^{*1}$ triplet state even at room temperature.[14]

An important consequence of the twist about the Mo–Mo bond is the lowered symmetry, D_2, of the $Mo_2X_4P_4$ core, which is of D_{2h} or D_{2d} symmetry in the absence of such a twist. The lack of an improper axis of symmetry of any order makes the $Mo_2X_4P_4$ core chiral and the Mo^{4+} moiety an inherently dissymmetric chromophore.[15]

All the molecules listed in Table I can exist as any of three enantiomeric pairs of conformers. These can be designated δΔδ, λΔλ, δΔδ, λΔλ, ΛΔδ, and δΔλ, where δ/λ refers to the sign of the P–C–C–P torsion angles in the two diphosphine ligands and Δ/Λ refers to the sign of the ϕ angle.

The compound β-$Mo_2Cl_4(dmpe)_2$ is spontaneously resolved and crystallizes in the enantiomorphous space group $P2_12_12$ or $P42_12$. However, the crystal structures are disordered and the conformers δΛδ and δΔδ are present in the crystals in unequal amounts. Rapid racemization on dissolution makes it impossible to study the optical activity of this compound in solution. In order to observe the optical activity of the dissymetric Mo_2^{4+} chromophore, it is thus necessary to stabilize one of the six types of conformers of a β-$Mo_2X_4(PP)_2$ molecule relative to the others. This can be done by using a chiral diphosphine ligand like (2*S*,3*S*)-bis(diphenylphosphino)butane. The circular dichroism spectrum of β-$Mo_2Cl_4(S,S\text{-dppb})_2$ was reported in a preliminary communication by the present authors.[6] We now report the structures of this compound and its bromo analogue and present a full interpretation of the CD spectra.

The electronic structure of the model compound $Mo_2Cl_4(PH_3)_4$ has been calculated by the SCF–Xα–SW method[16] and the HFS–LCAO method.[17] The effect of rotating the halves of the dimer relative to each other, about the Mo–Mo bond, on the electronic structure of the $Mo_2X_4P_4$ core is shown in Figure 1. This qualitative picture has been confirmed by SCF–Xα–SW

(1) (a) Texas A&M University. (b) The University of Glasglow.
(2) Cotton, F. A.; Powell, G.L. *Inorg. Chem.* **1983**, *22*, 1507.
(3) Campbell, F. L., III; Cotton, F. A.; Powell, G. L. *Inorg. Chem.* **1985**, *24*, 177.
(4) Agaskar, P. A.; Cotton, F. A. *Inorg. Chem.* **1984**, *23*, 3883.
(5) Agaskar, P. A. Ph.D Dissertation, Texas A&M University, 1985.
(6) Agaskar, P. A.; Cotton, F. A.; Fraser, I. F.; Peacock, R. D. *J. Am. Chem. Soc.* **1984**, *106*, 1851.
(7) DeCanio, E. C.; Cotton, F. A., unpublished work.
(8) Campbell, F. L., III; Cotton, F. A.; Powell, G. L. *Inorg. Chem.* **1985**, *24*, 4384.
(9) Abbott, E. H.; Bose, K. S.; Cotton, F. A.; Hall, W. T.; Sekutowski, J. C. *Inorg. Chem.* **1978**, *17*, 3240.
(10) Agaskar, P. A.; Cotton, F. A. *Rev. Chim. Miner.* **1985**, *22*, 302.
(11) Campbell, F. L., III; Cotton, F. A.; Powell, G. L. *Inorg. Chem.* **1984**, *23*, 4222.
(12) Cotton, F. A.; Extine, M. W.; Felthouse, T. R.; Kolthammer, B. W. S.; Lay, D. G. *J. Am. Chem. Soc.* **1981**, *103*, 4040.
(13) Cotton, F. A.; Fanwick, P. E.; Fitch, J. W.; Glicksman, H. D.; Walton, R. A. *J. Am. Chem. Soc.* **1979**, *101*, 1752.
(14) Hopkins, M. D.; Zietlow, T. C.; Miskowski, V. M.; Gray, H. B. *J. Am. Chem. Soc.* **1985**, *107*, 510.
(15) *Molecular Optical Activity and Chiral Discrimination*; Mason, S. F., Ed.; Cambridge University Press: New York, 1982.
(16) Cotton, F. A.; Hubbard, J. L.; Lichtenberger, D. L.; Shim, I. S. *J. Am. Chem. Soc.* **1982**, *104*, 679.
(17) Ziegler, T. *J. Am. Chem. Soc.* **1984**, *106*, 5901.

0020-1669/86/1325-2511$01.50/0

Table I. Complexes of the Type β-$Mo_2X_4(PP)_2$

compd	reactants	solvent	temp, time[b]	structure	ref
β-$Mo_2Cl_4(dmpe)_2$	$Mo_2Cl_4(PEt_3)_4$, dmpe	toluene	reflux, 12	D_2; $P2_12_12$, $P4_22_12$	2, 3
β-$Mo_2Cl_4(dppe)_2$	$Mo_2(O_2CCF_3)_4$, dppe, Me_3SiCl	THF	RT, 24	D_2; $P2_1/n$	4, 5
β-$Mo_2Cl_4(S,S\text{-dppb})_2$	$Mo_2(O_2CCF_3)_4$, *S,S*-dppb, Me_3SiCl	THF	RT, 24	D_2; $P2_12_12_1$	5, 6
β-$Mo_2Cl_4(dpcp)_2$	$K_4Mo_2Cl_8$, dpcp	MeOH	reflux, 6	D_2; $C2/c$	7
β-$Mo_2Cl_4(depe)_2$	$Mo_2Cl_4(PEt_3)_4$, depe	toluene	reflux, 12	D_2; $I4/mmm$	8
β-$Mo_2Cl_4(dppm)_2$	$K_4Mo_2Cl_8$, dppm	MeOH	reflux, 2	D_{2h}; $C2/c$	9
β-$Mo_2Br_4(dmpe)_2$	$Mo_2Br_4(PEt_3)_4$, dmpe	toluene	reflux, 20	D_2; $P2_12_12_1$	3
β-$Mo_2Br_4(dppe)_2$	$Mo_2(O_2CCF_3)_4$, dppe, Me_3SiBr	THF	RT, 12	D_2; $P2_1/n$	10
β-$Mo_2Br_4(S,S\text{-dppb})_2$	$Mo_2(O_2CCF_3)_4$, *S,S*-dppb, Me_3SiBr	THF	RT, 6	D_2; $P2_1$	5
β-$Mo_2Br_4(dpcp)_2$	$Mo_2(O_2CCF_3)_4$, dpcp, Me_3SiBr	THF	reflux, 6	D_2; $C2/c$	7
β-$Mo_2Br_4(dppm)_2$	$Mo_2(O_2CCH_3)_4$, dppm, Me_3SiBr	THF	reflux, 6	D_{2h}; $P2_1/n$	11

[a] Abbreviations: dmpe = $(CH_3)_2PCH_2CH_2P(CH_3)_2$; dppe = $(C_6H_5)_2PCH_2CH_2P(C_6H_5)_2$; dppm = $(C_6H_5)_2PCH_2P(C_6H_5)_2$; dpcp = $(C_6H_5)_2PCH(CH_2)_3CHP(C_6H_5)_2$; *S,S*-dppb = $(C_6H_5)_2PCH(CH_3)CH(CH_3)P(C_6H_5)_2$; dppe = $(C_2H_5)_2PCH_2CH_2P(C_2H_5)_2$. [b] RT = room temperature; time in units of h.

Table II. Important Bond and Torsion Angles in Compounds of the Type β-$Mo_2X_4(PP)_2$

X	PP	Mo–Mo–P, deg	Mo–Mo–X, deg	P–Mo–Mo–P, deg
Cl	$(C_6H_5)_2PCH_2CH_2P(C_6H_5)_2$	97.1 (4)	112.3 (7)	59.5
Cl	$(C_6H_5)_2PCH(CH_3)CH(CH_3)P(C_6H_5)_2$	103.8 (8)	107.4 (5)	24.7
Cl	$(C_6H_5)_2PCH(CH_2)_3CHP(C_6H_5)_2$	105.23 (8)	106.81 (9)	22.0
Cl	$(CH_3)_2PCH_2CH_2P(CH_3)_2$[a]	98.4 (2)	111.2 (9)	50.0
Cl	$(CH_3)_2PCH_2CH_2P(CH_3)_2$[b]	96.88 (8)	111.09 (7)	56.2
Cl	$(C_6H_5)_2PCH_2P(C_6H_5)_2$	99 (3)	106.9 (13)	0.0
Cl	$(CH_3)_3PP(CH_3)_3$	102.32 (2)	112.23 (2)	90.0
Br	$(C_6H_5)_2PCH_2CH_2P(C_6H_5)_2$	96.6 (4)	114.3 (3)	58.9
Br	$(C_6H_5)_2PCH(CH_3)CH(CH_3)P(C_6H_5)_2$	104.2 (2)	108.8 (2)	21.7
Br	$(C_6H_5)_2PCH(CH_2)_3CHP(C_6H_5)_2$	105.3 (1)	107.48 (8)	22.0
Br	$(CH_3)_2PCH_2CH_2P(CH_3)_2$	101.4 (3)	108.6 (3)	53.5
Br	$(C_6H_5)_2PCH_2(C_6H_5)_2$	99 (2)	108 (5)	0.0

[a] Orthorhombic. [b] Tetragonal.

Table III. Principal Bond Distances in Compounds of the Type β-$Mo_2X_4(PP)_2$

X	PP	M–M, Å	Mo–X, Å	Mo–P, Å
Cl	$(C_6H_5)_2PCH_2CH_2P(C_6H_5)_2$	2.183 (3)	2.385 (7)	2.579 (8)
Cl	$(C_6H_5)_2PCH(CH_3)CH(CH_3)P(C_6H_5)_2$	2.147 (3)	2.400 (8)	2.566 (8)
Cl	$(C_6H_5)_2PCH(CH_2)_3CHP(C_6H_5)_2$	2.159 (2)	2.399 (3)	2.574 (4)
Cl	$(CH_3)_2PCH_2CH_2P(CH_3)_2$[a]	2.183 (3)	2.402 (5)	2.526 (5)
Cl	$(CH_3)_2PCH_2CH_2P(CH_3)_2$[b]	2.168 (1)	2.387 (2)	2.522 (3)
Cl	$(C_6H_5)_2PCH_2P(C_6H_5)_2$	2.138 (1)	2.394 (1)	2.584 (1)
Cl	$(CH_3)_3PP(CH_3)_3$	2.130 (0)	2.414 (1)	2.545 (1)
Br	$(C_6H_5)_2PCH_2CH_2P(C_6H_5)_2$	2.177 (8)	2.512 (8)	2.624 (14)
Br	$(C_6H_5)_2PCH(CH_3)CH(CH_3)P(C_6H_5)_2$	2.147 (6)	2.538 (8)	2.594 (15)
Br	$(C_6H_5)_2PCH(CH_2)_3CHP(C_6H_5)_2$	2.155 (4)	2.541 (2)	2.586 (7)
Br	$(CH_3)_2PCH_2CH_2P(CH_3)_2$	2.169 (2)	2.545 (2)	2.536 (5)
Br	$(C_6H_5)_2PCH_2P(C_6H_5)_2$	2.138 (1)	2.534 (1)	2.611 (2)

[a] Orthorhombic. [b] Tetragonal.

calculations of the electronic structures of several conformers of the model compound $Mo_2Cl_4(PH_3)_4$, the results of which will be published elsewhere.

The band at lowest energy in the electronic absorption spectra of these compounds has been definitively assigned to the $\delta_{xy} \rightarrow \delta^*_{xy}$ transition.[18,19] The next band at higher energy was tentatively assigned to a $\pi \rightarrow \delta^*$ transition[6] on the basis of assignments made in the absorption spectrum of $K_4Mo_2Cl_8$.[20,21] The first strong band in the UV region that had an energy close to that of the band assigned to a $\pi \rightarrow \delta_{x^2-y^2}$ transition in $K_4Mo_2Cl_8$ was believed to be a phosphine to metal charge-transfer band.[14]

These last assignments have been revised in light of the calculations mentioned above and the experimentally observed shifts in the bond positions resulting from atom substitutions and changes in the ϕ angle. The discussion at the end of this paper shows how an analysis of transition densities of each of these proposed assignments can give predicted signs that are consistent with the signs of the bands in the observed spectra.

Experimental Procedures

The compounds $Mo_2(O_2CCF_3)_4$ and $K_4Mo_2Cl_8$ were prepared by methods described in the literature.[22,23] The ligand (2*S*,3*S*)-bis(diphenylphosphino)butane (*S,S*-dppb) was purchased from Strem Chemicals, Inc.

All solvents used were dried and freed of oxygen by refluxing over the appropriate reagent. All reactions were carried out in Schlenk-type glassware under an atmosphere of pure N_2.

Preparation A. $Mo_2(O_2CCF_3)_4$ (40 mg) was dissolved in THF (5 mL), and Me_3SiCl (0.1 mL) was added. The solution was stirred for 12 h, and *S,S*-dppb (53 mg) was then added. The orange solution turned red immediately and was allowed to stand for 1 day. A yellow-green solution was obtained. The solvent was removed under reduced pressure to give a green powder, which was washed with anhydrous ether and dried in vacuo. The solid was extremely soluble in THF, MeOH, EtOH, CH_3CN, CH_2Cl_2, C_5H_6, and $C_6H_5CH_3$. The solutions were all air-sensitive, but the solid itself was air-stable.

The visible absorption spectrum of a THF solution of the green β-$Mo_2Cl_4(S,S\text{-dppb})_2$ had bands at 740, 470, and 362 nm. The far-IR

(18) Cowman, D.; Trogler, W. C.; Gray, H. B. *Isr. J. Chem.* **1976**, *15*, 308.
(19) Cotton, F. A. *Coord. Chem.* **1981**, *21*, 11.
(20) Norman, J. G., Jr.; Kolari, H. J. *J. Am. Chem. Soc.* **1975**, *97*, 33.
(21) Fanwick, P. E.; Martin, D. E.; Cotton, F. A.; Webb, T. R. *Inorg. Chem.* **1977**, *16*, 2103.
(22) Cotton, F. A.; Norman, J. G., Jr. *J. Coord. Chem.* **1971**, *1*, 161.
(23) Brencic, J. V.; Cotton, F. A. *Inorg. Chem.* **1970**, *9*, 351.

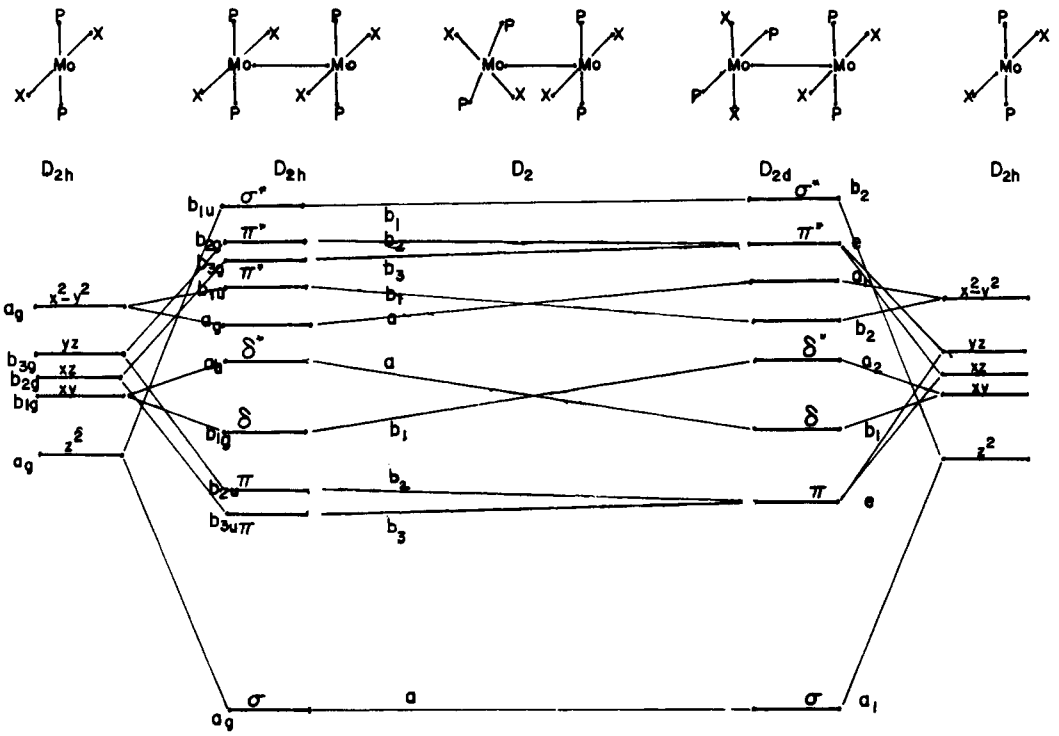

Figure 1. Qualitative MO diagram of molecules of the type β-$Mo_2X_4(PP)_2$.

spectrum had peaks at 335 and 275 cm^{-1}.

Crystals suitable for X-ray diffraction measurements were obtained by hexane-induced crystallization from a THF solution.

Preparation B. $K_4Mo_2Cl_8$ (80 mg) was mixed with *S,S*-dppb (106 mg), and MeOH (5 mL) was added. The mixture was then refluxed for a few hours until all the red starting material had disappeared, leaving a green solid and a yellow-green solution. The MeOH was removed by filtration and the residue washed with more MeOH, followed by anhydrous ether. It was dried under vacuum.

The green powder was identical with the product of preparation A. Crystals suitable for X-ray diffraction measurements were obtained by recrystallization from CH_3CN.

Preparation C. $Mo_2(O_2CCF_3)_4$ (40 mg) was dissolved in THF (5 mL), and Me_3SiBr (0.15 mL) was added, followed by *S,S*-dppb (53 mg). The mixture was stirred for a few hours until a dark green solution was obtained. The solvent was removed under reduced pressure and the green residue washed with hexane. The green solid, β-$Mo_2Br_4(S,S\text{-dppb})_2$, was soluble in all solvents mentioned in preparation A and was air-stable. The electronic absorption spectrum of a solution in THF had band maxima at 765, 490, and 380 nm. A far-IR spectrum showed a weak peak at 265 cm^{-1}.

Single crystals suitable for X-ray diffraction measurements were obtained by recrystallization from a THF solution at low temperatures.

X-ray Data Collection. β-$Mo_2Cl_4(S,S\text{-dppb})_2\cdot C_4H_8O$. A green crystal of dimensions 0.3 × 0.2 × 0.2 mm was mounted in a glass capillary, and its unit cell constants were determined from 25 reflections with 2θ values in the range 10–25°. These were consistent with a primitive orthorhombic lattice, and the space group was subsequently determined to be $P2_12_12_1$ from systematic absences. All relevant crystallographic data are listed in Table IV.

Intensities of all reflections with 2θ values in the range 4.0–50.0° were measured by ω–2θ scans. The total number of reflections measured was 6537, of which 345 were intensity standards. The data were corrected for Lorentz and polarization effects. No absorption corrections were applied as the linear absorption coefficient was only 7 cm^{-1}.

β-$Mo_2Cl_4(S,S\text{-dppb})_2\cdot 4CH_3CN$. The specimen used was a green needle, 0.75 × 0.25 × 0.25 mm, mounted in a quartz capillary and submerged in acetonitrile. X-ray measurements were made with X-rays on an Enraf-Nonius CAD-4F diffractometer equipped with a graphite monochromator. Cell dimensions were derived from the settings of 25 automatically centered reflections. The space group was determined from the observed Laue symmetry and systematic absences.

The intensities were measured from continuous $\theta/2\theta$ scans. They were corrected for Lorentz and polarization effects, variation (<10%) in the intensities of standard reflections, and absorption. All subsequent calculations employed only the independent reflections for which $I > 1.5\sigma(I)$. All pertinent crystallographic data are listed in Table V.

β-$Mo_2Br_4(S,S\text{-dppe})_2\cdot {}^1/_2C_4H_8O$. A green plate-like crystal of dimensions 0.5 × 0.5 × 0.2 mm was sealed inside a thin-walled glass capillary with epoxy cement. The unit cell constants were consistent with a primitive monoclinic lattice, and the space group was determined to be $P2_1$ from systematic absences. A summary of all relevant crystallographic data is presented in Table IV.

The intensities of all reflections with 2θ values in the range 5.0–50.0° were measured by ω–2θ scans. The total number of reflections measured was 7402, of which 277 were intensity standards. Lorentz and polarization corrections were made, and an empirical absorption correction was applied based on azimuthal scans of nine reflections with χ angles near 90°.

Solution and Refinement of Structures. β-$Mo_2Cl_4(S,S\text{-dppb})_2\cdot C_4H_8O$. The structure was solved with use of direct methods to determine the positions of the two independent molybdenum atoms. The remaining atoms were found in a series of difference Fourier maps alternating with least-squares refinement of the atoms found. Anisotropic thermal parameters were used only for Mo, Cl, and P atoms. The isotropic thermal parameters of chemically equivalent carbon atoms in the ligands and all carbon atoms in the solvent molecule were constrained to be equal. The eight phenyl rings were constrained to $6/mmm$ symmetry with C–C = 1.395 Å. Equivalent P–C and C–C bond lengths were refined as free variables. The correct enantiomer was chosen by requiring the diphosphine ligand to be in the *S,S* form.

Refinement of this model gave a final *R* factor of 0.0767. This and other relevant details of the refinement are listed in Table IV. The final positional parameters and the isotropic (equivalent) thermal parameters are listed in Tables VI and VI-S (supplementary material).

β-$Mo_2Cl_4(S,S\text{-dppb})_2\cdot 4CH_3CN$. The non-hydrogen atoms were located by Patterson and difference Fourier methods. Their parameters were refined by full-matrix least-squares minimization of $\sum w(|F_o| - |F_c|)^2$.

In the final calculations anisotropic thermal parameters were used only for Mo, Cl, and P atoms. The eight phenyl rings were constrained to have $6/mmm$ symmetry with C–C = 1.38 Å. The scattering of the hydrogen atoms, apart from those of acetonitrile molecules, was included in the structure factor calculations. The hydrogen atoms were constrained to ride on adjacent carbon atoms with C–H = 1.0 Å and *U*(H) = *U*(C). The absolute configuration was checked by refining the Rogers chirality parameter, η, from −1.0.[24] The final η value was 1.21 (17), with $(1 + |\eta|)/\sigma(\eta) = 13.2$, confirming that the complex contains the *S,S* form of the 2,3-bis(diphenylphosphino)butane ligand. The final *R* factor was 0.068. This and all other pertinent details are listed in Table V. The

(24) Rogers, D. *Acta Crystallogr., Sect. A: Cryst. Phys., Diffr., Theor. Gen. Crystallogr.* **1981**, *A37*, 734.

Table IV. Crystallographic Data from Texas A&M University for Two β-$Mo_2X_4(S,S\text{-dppb})_2$ Compounds

formula	$Mo_2Cl_4((C_6H_5)_2PCH(CH_3)CH(CH_3)P(C_6H_5)_2)_2 \cdot OC_4H_8$	$Mo_2Br_4((C_6H_5)_2PCH(CH_3)CH(CH_3)P(C_6H_5)_2)_2$
fw	1258.75	1364.48
space group	$P2_12_12_1$	$P2_1$
systematic absences	$h00$, $h \neq 2n$; $0k0$, $k \neq 2n$; $00l$, $l \neq 2n$	$0k0$, $k \neq 2n$
a, Å	14.57 (1)	16.78 (1)
b, Å	36.69 (1)	16.98 (1)
c, Å	11.84 (1)	27.19 (1)
α, deg	90.0	90.0
β, deg	90.0	97.35 (3)
γ, deg	90.0	90.0
V, Å^3	6329 (12)	7685 (9)
Z	4	4
d_{calcd}, g/cm^3	1.320	1.179
cryst size, mm	0.3 × 0.2 × 0.2	0.2 × 0.5 × 0.5
μ(Mo Kα), cm^{-1}	6.932	24.861
data collection instrument	Enraf-Nonius CAD-4	Syntex P$\bar{1}$
radiation (monochromated in incident beam)	Mo Kα	Mo Kα
orientation reflecns: no. range (2θ), deg	25, $10 < 2\theta < 25$	15, $15 < 2\theta < 25$
temp, °C	22 ± 3	22 ± 3
scan method	$\omega/2\theta$	$\omega/2\theta$
data collecn range, 2θ, deg	$4.0 \leq 2\theta \leq 50.0$	$5.0 \leq 2\theta \leq 50.0$
no. of unique data, total with $F_o > 3\sigma(F_o^2)$	6183, 2314	7271, 3811
no. of params refined	193	362
transmission factors: max, min		99.75, 70.77%
R^a	0.0767	0.0788
R_w^b	0.0986	0.1090
quality of fit indicator^c	1.52	1.160
largest shift/esd, final cycle	0.02	0.09
largest peak, e/Å^3	0.73	0.82

$^a R = \sum||F_o| - |F_c||/\sum|F_o|$. $^b R_w = [\sum w(|F_o| - |F_c|)^2/\sum w|F_o|^2]^{1/2}$; $w = 1/\sigma^2(|F_o|)$. ^{c}Quality of fit $= [\sum w(|F_o| - |F_c|)^2/(N_{observns} - N_{params})]^{1/2}$.

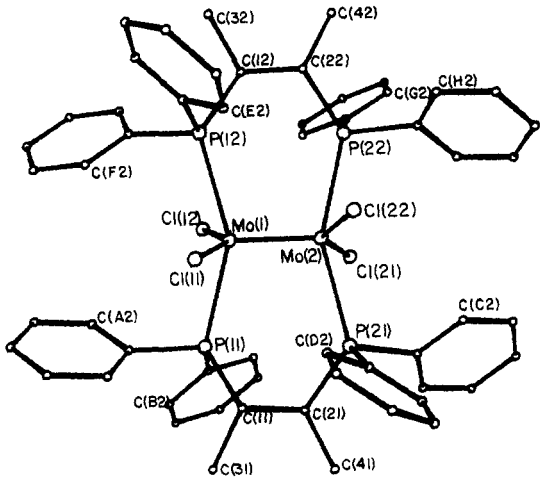

Figure 3. View of the entire molecule of β-$Mo_2Cl_4(S,S\text{-dppb})_2$ showing the atom-labeling scheme used in the crystal structure of the CH_3CN solvate.

final positional parameters and isotropic thermal parameters of the non-hydrogen atoms are listed in Table VII.

β-$Mo_2Br_4(S,S\text{-dppb})_2 \cdot {}^1/_2C_4H_8O$. The position of one of the molybdenum atoms was determined from a Patterson map. The positions of the rest of the atoms were determined from difference Fourier maps. Two independent molecules of β-$Mo_2Cl_4(S,S\text{-dppb})_2$ were found in the asymmetric unit. The constraints applied were similar to those used in the other structures. The total number of parameters refined was 193. Refinement of this model gave an R factor of 0.0788. This and all other relevant details are listed in Table IV. The final positional parameters and isotropic (equivalent) thermal parameters are listed in Tables VIII and VIII-S (supplementary material).

Results

The compound β-$Mo_2Cl_4(S,S\text{-dppb})_2$ crystallizes in the enantiomorphic space group $P2_12_12_1$ and with 4 molecules of THF included in the unit cell in one case and 16 molecules of CH_3CN in the other.

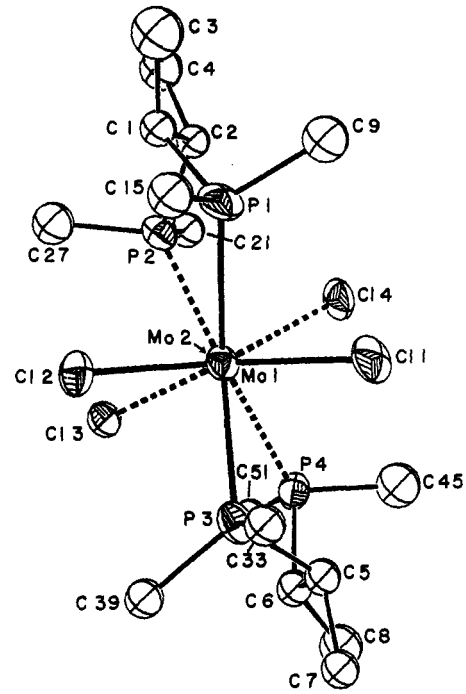

Figure 4. View of the molecule of β-$Mo_2Cl_4(S,S\text{-dppb})_2$ down the Mo$\equiv$Mo bond.

The entire molecules are shown in Figures 2 and 3. A view down the Mo(1)–Mo(2) axis is shown in Figure 4. The Mo$\equiv$Mo bond lengths in the two crystals are 2.147 (3) and 2.144 (2) Å, respectively. These are listed along with the other principal bond distances and bond angles in Tables IX and X. The molecules in both crystals approximate to D_2 symmetry. The two six-membered rings Mo–P–C–C–P–Mo have a conformation that can best be described as a distorted chair. The average P–C–C–P torsion angles are different in the two crystals, 76.2 [1] and 69.4

Table V. Crystallographic Data from the University of Glasgow for Mo_2Cl_4(S,S-dppb)$_2$·4CH_3CN

compound	$[Mo_2Cl_4(Ph_2PCHMeCHMePPh_2)_2]$·4$CH_3CN$
formula	$C_{64}H_{68}Cl_4Mo_2N_4P_4$
fw	1350.9
cryst syst	orthorhombic
space group	$P2_12_12_1$
unit cell constants	
a, Å	13.535 (3)
b, Å	21.044 (7)
c, Å	23.214 (3)
V, Å^3	6612 (6)
Z	4
F(000), e	2768
d_{calcd}, g/cm^3	1.357
temp, °C[a]	20
radiation	Mo Kα, λ = 0.71069 Å (graphite monochromated)
μ(Mo Kα), cm^{-1}	6.7
abs factors (on *F*)	0.85–1.05
intens measmts	
scan type	θ/2θ
scan width (Δω), deg	0.90
max counting time, s	120
reflecns measd	7434
2θ	4–53
q[b]	0.05
final refinement	
no. of unique reflecns with $I > 1.5\sigma(I)$	4753
no. of variables[c]	314
largest param shift/error	0.74
mean param shift/error	0.05
R[d]	0.068
R_w[b]	0.063
least-squares wts (*w*)	$\sigma^2(F)$
esd, e[e]	1.64
$\lvert\Delta\rho\rvert$, e/Å^3[f]	0.83

[a] Temperature at which the diffraction measurements were carried out. [b] Manojlović-Muir, Lj.; Muir, K. W. *J. Chem. Soc., Dalton Trans.* **1974**, 2427–2433. [c] 269 structure parameters and 45 defining the empirically derived transmission surface. [d] $R = \sum(|F_o| - |F_c|)/\sum|F_o|$; $R_w = [\sum w(|F_o| - |F_c|)^2/\sum w|F_o|^2]^{1/2}$. [e] Error in observation of unit weight. [f] Extreme function value in the final difference Fourier synthesis.

(8)°, respectively, but the P–Mo–Mo–P torsion angles are virtually the same, 24 [2] and 22 [1]°, respectively. The observed conformer, designated δΛδ, is the expected one, since it puts the methyl groups in equatorial positions when the configuration at the chiral carbon atoms is *S*.

The compound β-Mo_2Br_4(S,S-dppb)$_2$ crystallizes in space group $P2_1$. There are two independent molecules in the asymmetric unit, the structures of which are almost exactly the same and similar to the structure of β-Mo_2Cl_4(S,S-dppb)$_2$. Figure 5 gives a view of one of the molecules down the Mo(1)–Mo(2) bond and can be compared with Figure 4. The atom-labeling scheme for the second molecule is similar to that shown here.

The Mo(1)–Mo(2) and Mo(3)–Mo(4) bond distances are 2.147 (6) and 2.152 (6) Å, respectively, not significantly different from each other nor from the Mo(1)–Mo(2) bond distance of 2.147 (3) Å in the chloro analogue. The average P–Mo–Mo–P torsion angle is 21.7 [4]°, which is slightly smaller than the corresponding angle in the chloro analogue. Important bond distances and bond angles are listed in Table XI.

The absorption and CD spectra of the chloride and bromide complexes are shown in Figures 6–9. The absorption spectra show the usual three bands characteristic of bridged $Mo_2X_4(PP)_2$ complexes, at 740, 470, and 370 nm in Mo_2Cl_4(S,S-dppb)$_2$ and at 760, 490, and 380 nm in Mo_2Br_4(S,S-dppb)$_2$. The CD spectra, however, show the presence of four more transitions, which are either extremely weak in the absorption spectra or are hidden under the high-energy tails. All the transitions for both complexes are listed in Table XII along with the signs and magnitudes of the associated CD features. The lowest energy absorption in quadruply bonded dimolybdenum complexes is invariably due to the $\delta_{xy} \rightarrow \delta^*_{xy}$ transition, and the calculations performed[5] for the twisted $Mo_2X_4P_4$ chromophore agree with this assignment. We start, therefore, by describing a model to account for the sign of the CD of the $\delta_{xy} \rightarrow \delta^*_{xy}$ transition and proceed to discuss the rest of the spectra.

Table VI. Positional Parameters and Isotropic Thermal Parameters for β-Mo_2Cl_4(S,S-dppb)$_2$·THF[a]

atom	*x*	*y*	*z*	*B*, Å^2
Mo(1)	0.6775 (2)	0.85164 (6)	0.5464 (2)	2.89 (6)
Mo(2)	0.6931 (2)	0.88173 (6)	0.3920 (2)	2.63 (6)
Cl(1)	0.5621 (6)	0.8065 (2)	0.5105 (8)	4.6 (2)
Cl(2)	0.7759 (5)	0.8788 (2)	0.6858 (6)	3.5 (2)
Cl(3)	0.7533 (5)	0.9407 (2)	0.4374 (7)	3.6 (2)
Cl(4)	0.6519 (6)	0.8416 (2)	0.2400 (7)	4.4 (2)
P(1)	0.7936 (6)	0.7994 (2)	0.5258 (7)	4.5 (2)
P(2)	0.8569 (5)	0.8675 (2)	0.3285 (7)	3.3 (2)
P(3)	0.5449 (5)	0.8824 (2)	0.6530 (6)	3.3 (2)
P(4)	0.5321 (5)	0.9093 (2)	0.3671 (7)	3.5 (2)
O(1)	0.863 (3)	0.484 (1)	0.346 (4)	19 (1)*
C(1)	0.909 (1)	0.8077 (7)	0.458 (2)	4.0 (3)*
C(2)	0.896 (2)	0.8185 (5)	0.334 (2)	4.0 (3)*
C(3)	0.966 (2)	0.7701 (7)	0.467 (3)	5.3 (4)*
C(4)	0.991 (2)	0.8138 (9)	0.264 (3)	5.3 (4)*
C(5)	0.438 (1)	0.8907 (7)	0.566 (2)	4.0 (3)*
C(6)	0.456 (2)	0.9234 (7)	0.489 (2)	4.0 (3)*
C(7)	0.353 (2)	0.8995 (8)	0.649 (3)	5.3 (4)*
C(8)	0.361 (2)	0.9389 (8)	0.437 (3)	5.3 (4)*
C(9)	0.753 (1)	0.7555 (4)	0.467 (2)	4.2 (2)*
C(15)	0.818 (2)	0.7876 (5)	0.6746 (9)	4.2 (2)*
C(27)	0.959 (1)	0.8916 (5)	0.384 (2)	4.2 (2)*
C(33)	0.517 (2)	0.8497 (5)	0.767 (1)	4.2 (2)*
C(39)	0.560 (2)	0.9254 (4)	0.732 (2)	4.2 (2)*
C(45)	0.453 (1)	0.8855 (6)	0.270 (2)	4.2 (2)*

[a] For the atoms depicted in Figure 4. A view of the entire molecule and a complete set of positional parameters are available in the supplementary material. Values marked with an asterisk indicate that the associated were refined isotropically. Anistropically refined atoms are given in the form of the isotropic equivalent thermal parameter defined as $^4/_3[a^2\beta_{11} + b^2\beta_{22} + c^2\beta_{33} + ab(\cos\gamma)\beta_{12} + ac(\cos\beta)\beta_{13} + bc(\cos\alpha)\beta_{23}]$.

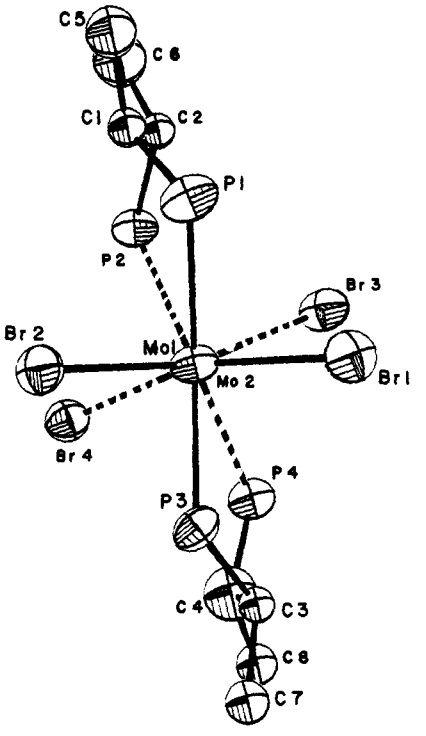

Figure 5. View of the molecule of β-Mo_2Br_4(S,S-dppb)$_2$ down the Mo–Mo bond. The atom-labeling scheme shown in here is for one of the molecules in the asymmetric unit.

Table VII. Fractional Coordinates and Isotropic Vibrational Parameters for Non-Hydrogen Atoms in $[Mo_2Cl_4(Ph_2PCHMeCHMePPh_2)_2]\cdot 4CH_3CN$

	x/a	y/b	z/c	U,[a] Å²		x/a	y/b	z/c	U,[a] Å²
Mo(1)	0.15140 (6)	−0.22062 (4)	0.22859 (3)	0.0311 (5)	C(D4)	−0.0226 (7)	0.0534 (4)	0.3705 (6)	0.066 (4)
Mo(2)	0.22952 (6)	−0.19134 (4)	0.30443 (4)	0.0337 (5)	C(D5)	−0.0041 (10)	0.0236 (4)	0.4223 (4)	0.064 (3)
Cl(11)	0.0809 (2)	−0.1263 (1)	0.1874 (1)	0.0441 (16)	C(D6)	0.0355 (6)	−0.0368 (5)	0.4230 (4)	0.056 (3)
Cl(12)	0.1609 (2)	−0.3341 (1)	0.2214 (1)	0.0441 (15)	C(E1)	0.2895 (5)	−0.1419 (4)	0.1065 (4)	0.044 (3)
Cl(21)	0.2450 (2)	−0.2821 (2)	0.3662 (1)	0.0524 (17)	C(E2)	0.2961 (9)	−0.0849 (6)	0.1357 (3)	0.051 (3)
Cl(22)	0.2718 (2)	−0.0813 (1)	0.2908 (1)	0.0499 (16)	C(E3)	0.3077 (11)	−0.0289 (5)	0.1056 (5)	0.069 (4)
P(11)	−0.0250 (2)	−0.2427 (1)	0.2650 (1)	0.0344 (16)	C(E4)	0.3127 (5)	−0.0298 (4)	0.0462 (4)	0.084 (4)
P(12)	0.2849 (2)	−0.2141 (1)	0.1494 (1)	0.0405 (17)	C(E5)	0.3061 (9)	−0.0868 (6)	0.0170 (3)	0.100 (5)
P(21)	0.0926 (2)	−0.1509 (1)	0.3719 (1)	0.0357 (16)	C(E6)	0.2945 (11)	−0.1428 (5)	0.0472 (5)	0.061 (3)
P(22)	0.4109 (2)	−0.2127 (2)	0.2819 (1)	0.049 (2)	C(F1)	0.2468 (13)	−0.2755 (7)	0.0977 (4)	0.053 (3)
C(11)	−0.0858 (7)	−0.1890 (5)	0.3186 (4)	0.037 (2)	C(F2)	0.1578 (11)	−0.2646 (4)	0.0705 (7)	0.070 (4)
C(21)	−0.0312 (7)	−0.1896 (5)	0.3760 (4)	0.041 (2)	C(F3)	0.1209 (7)	−0.3088 (8)	0.0321 (6)	0.100 (5)
C(31)	−0.1932 (8)	−0.2079 (6)	0.3250 (5)	0.054 (3)	C(F4)	0.1732 (13)	−0.3638 (7)	0.0210 (4)	0.102 (6)
C(41)	−0.0909 (9)	−0.1629 (6)	0.4264 (5)	0.059 (3)	C(F5)	0.2622 (11)	−0.3746 (4)	0.0483 (7)	0.101 (5)
C(12)	0.4204 (8)	−0.2305 (6)	0.1632 (5)	0.053 (3)	C(F6)	0.2990 (7)	−0.3304 (8)	0.0866 (6)	0.082 (4)
C(22)	0.4631 (9)	−0.1888 (6)	0.2110 (5)	0.059 (3)	C(G1)	0.4604 (9)	−0.2932 (4)	0.2907 (6)	0.050 (3)
C(32)	0.4776 (10)	−0.2201 (7)	0.1053 (6)	0.076 (4)	C(G2)	0.5517 (11)	−0.3034 (6)	0.3154 (3)	0.074 (4)
C(42)	0.5785 (11)	−0.1958 (7)	0.2096 (6)	0.079 (4)	C(G3)	0.5912 (6)	−0.3638 (8)	0.3169 (6)	0.089 (5)
C(A1)	−0.0956 (8)	−0.2364 (7)	0.1978 (4)	0.041 (2)	C(G4)	0.5393 (9)	−0.4141 (4)	0.2936 (6)	0.094 (5)
C(A2)	−0.0821 (6)	−0.2847 (5)	0.1584 (6)	0.056 (3)	C(G5)	0.4480 (11)	−0.4039 (6)	0.2688 (3)	0.076 (4)
C(A3)	−0.1265 (10)	−0.2813 (4)	0.1050 (4)	0.078 (4)	C(G6)	0.4086 (6)	−0.3434 (8)	0.2673 (6)	0.063 (3)
C(A4)	−0.1844 (8)	−0.2296 (7)	0.0910 (4)	0.072 (4)	C(H1)	0.4747 (14)	−0.1656 (8)	0.3372 (4)	0.060 (3)
C(A5)	−0.1978 (6)	−0.1813 (5)	0.1304 (6)	0.060 (3)	C(H2)	0.5155 (9)	−0.1072 (8)	0.3242 (4)	0.093 (5)
C(A6)	−0.1535 (10)	−0.1847 (4)	0.1838 (4)	0.049 (3)	C(H3)	0.5554 (9)	−0.0702 (4)	0.3674 (5)	0.139 (8)
C(B1)	−0.0527 (6)	−0.3229 (3)	0.2931 (4)	0.041 (3)	C(H4)	0.5545 (14)	−0.0915 (8)	0.4236 (4)	0.138 (8)
C(B2)	−0.1335 (5)	−0.3579 (7)	0.2756 (5)	0.050 (3)	C(H5)	0.5137 (9)	−0.1499 (8)	0.4366 (4)	0.088 (5)
C(B3)	−0.1522 (8)	−0.4164 (6)	0.3002 (3)	0.068 (3)	C(H6)	0.4738 (9)	−0.1869 (4)	0.3935 (5)	0.076 (4)
C(B4)	−0.0901 (6)	−0.4399 (3)	0.3422 (4)	0.073 (4)	N(S1)	0.901 (2)	0.035 (1)	0.605 (1)	0.211 (11)
C(B5)	−0.0093 (5)	−0.4049 (7)	0.3597 (5)	0.064 (4)	N(S2)	0.439 (2)	0.112 (1)	0.395 (1)	0.248 (15)
C(B6)	0.0094 (8)	−0.3464 (6)	0.3352 (3)	0.052 (3)	N(S3)	0.113 (2)	0.487 (1)	0.454 (1)	0.170 (8)
C(C1)	0.1541 (7)	−0.1592 (7)	0.4425 (4)	0.044 (3)	N(S4)	0.681 (2)	−0.012 (1)	0.691 (1)	0.166 (10)
C(C2)	0.2322 (4)	−0.1187 (4)	0.4531 (4)	0.054 (3)	C(S1)	0.888 (3)	−0.014 (2)	0.582 (1)	0.204 (13)
C(C3)	0.2856 (8)	−0.1241 (6)	0.5035 (3)	0.061 (3)	C(S2)	0.850 (3)	−0.077 (2)	0.568 (1)	0.227 (14)
C(C4)	0.2608 (7)	−0.1701 (7)	0.5433 (4)	0.072 (4)	C(S3)	0.379 (2)	0.102 (2)	0.374 (1)	0.172 (11)
C(C5)	0.1827 (4)	−0.2106 (4)	0.5328 (4)	0.079 (4)	C(S4)	0.296 (2)	0.064 (1)	0.351 (1)	0.176 (10)
C(C6)	0.1294 (8)	−0.2052 (6)	0.4824 (3)	0.071 (4)	C(S5)	0.544 (2)	0.052 (1)	0.543 (1)	0.142 (8)
C(D1)	0.0566 (7)	−0.0674 (4)	0.3719 (6)	0.038 (2)	C(S6)	0.479 (2)	0.105 (1)	0.537 (1)	0.136 (7)
C(D2)	0.0382 (10)	−0.0376 (4)	0.3201 (4)	0.045 (3)	C(S7)	0.730 (3)	0.019 (2)	0.723 (2)	0.243 (15)
C(D3)	−0.0015 (6)	0.0228 (5)	0.3194 (4)	0.063 (3)	C(S8)	0.247 (2)	0.451 (1)	0.226 (1)	0.227 (11)

[a] For Mo, Cl, and P atoms $U = (U_{11} + U_{22} + U_{33})/3$. For other atoms an isotropic temperature factor of the form $\exp(-8\pi^2 U(\sin^2\theta)/\lambda^2)$ was used.

CD of the $\delta_{xy} \rightarrow \delta^*_{xy}$ Transition. The $\delta_{xy} \rightarrow \delta^*_{xy}$ transition of the eclipsed $Mo_2X_4P_4$ chromophore has b_{1u} symmetry and is electric-dipole allowed with polarization along with Mo–Mo bond. The effect of twisting the complex about the Mo–Mo axis is to make the transition both electric- *and* magnetic-dipole allowed (b_1 symmetry in D_2). The magnetic- and electric-dipole transition moments are collinear, and so the $\delta_{xy} \rightarrow \delta^*_{xy}$ transition is optically active and shows CD. The net result of these collinear electric- and magnetic-dipole transition moments is a displacement of charge along and around the Mo–Mo bond, or, in other words, a helical displacement of charge. A left-handed helical charge displacement gives rise[15] to a negative CD or Cotton effect and a right-handed helical charge displacement to a positive CD. The sign of the CD can therefore be predicted if we can relate the handedness of the helical charge displacement to the geometry of the $Mo_2X_4P_4$ chromophore.

The top part of Figure 10 shows how one may obtain the transient charge distribution produced during the $\delta_{xy} \rightarrow \delta^*_{xy}$ transition for the twisted $Mo_2X_4P_4$ chromophore by multiplying the phases of the δ_{xy} orbitals. The direction of the charge movement may be seen by following the signs (from + to − or − to +) through the shortest spacial path and is clearly that of a helix directed along the Mo–Mo bond. The bottom part of Figure 10 shows the same transient charge displacement as one looks down the Mo–Mo bond for the Λ absolute configuration and for twists of the P–Mo–Mo–P angle both less than and greater than 45°. In both cases the electric-dipole transition moment, μ, is along the metal–metal bond in the $+Z$ direction; the magnetic-dipole transition moment, m, however, is directed along the metal–metal bond in the $-Z$ direction when the twist angle is less

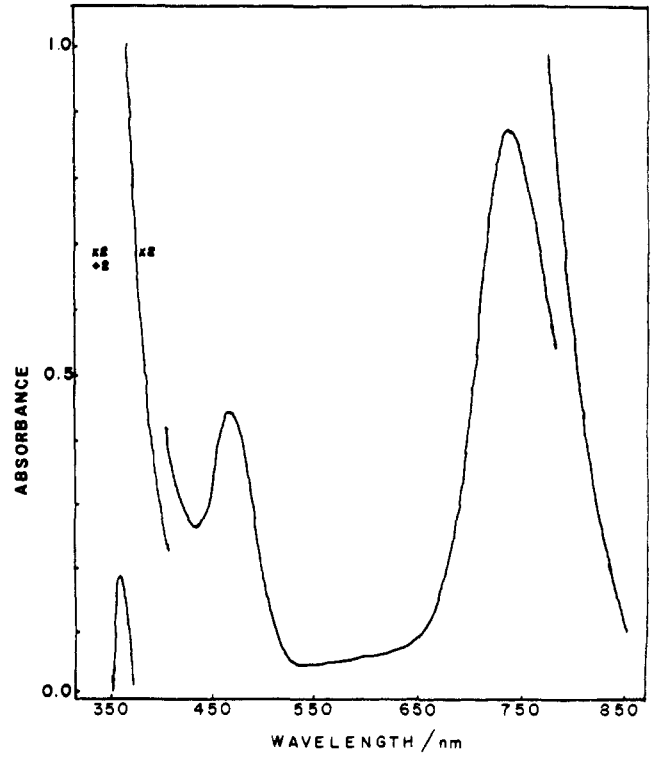

Figure 6. Electronic absorption spectrum of β-Mo_2Cl_4(*S*,*S*-dppb)$_2$ in THF solution (C = 0.06 mM, l = 1 cm).

Table VIII. Positional Parameters and Isotropic Thermal Parameters for β-$Mo_2Br_4(S,S\text{-dppb})_2$[a]

atom	x	y	z	B, Å²
Mo(1)	0.7661 (3)	0.750	0.9333 (2)	3.4 (1)
Mo(2)	0.7089 (3)	0.6367 (4)	0.9300 (2)	3.2 (1)
Mo(3)	0.2922 (2)	0.7545 (4)	0.4328 (2)	3.0 (1)
Mo(4)	0.1781 (2)	0.8118 (4)	0.4347 (2)	3.0 (1)
Br(1)	0.7807 (3)	0.8000 (5)	1.0219 (2)	4.5 (2)
Br(2)	0.7946 (3)	0.7891 (4)	0.8474 (2)	4.9 (2)
Br(3)	0.7277 (3)	0.5770 (4)	1.0164 (2)	4.4 (2)
Br(4)	0.6500 (3)	0.6114 (4)	0.8405 (2)	4.7 (2)
Br(5)	0.3677 (3)	0.7517 (5)	0.5203 (2)	4.3 (1)
Br(6)	0.3043 (3)	0.7156 (5)	0.3443 (2)	4.4 (2)
Br(7)	0.1408 (3)	0.8043 (5)	0.5217 (2)	4.4 (2)
Br(8)	0.1284 (3)	0.8608 (4)	0.3480 (2)	4.7 (2)
P(1)	0.9173 (8)	0.7162 (8)	0.9535 (5)	3.7 (4)
P(2)	0.8186 (8)	0.5377 (8)	0.9117 (5)	3.9 (4)
P(3)	0.6477 (9)	0.8496 (8)	0.9171 (5)	4.5 (4)
P(4)	0.5637 (8)	0.6671 (8)	0.9475 (5)	3.8 (4)
P(5)	0.2626 (7)	0.6090 (8)	0.4484 (5)	3.4 (4)
P(6)	0.0725 (8)	0.6991 (9)	0.4147 (5)	4.2 (4)
P(7)	0.3903 (7)	0.8686 (8)	0.4172 (5)	3.6 (4)
P(8)	0.2164 (7)	0.9557 (8)	0.4559 (5)	3.9 (4)
C(1)	0.966 (2)	0.631 (2)	0.927 (1)	3 (1)*
C(2)	0.924 (1)	0.553 (2)	0.939 (2)	7 (2)*
C(3)	0.552 (2)	0.832 (2)	0.942 (1)	3 (1)*
C(4)	0.509 (2)	0.755 (1)	0.922 (1)	2.7 (9)*
C(5)	1.058 (2)	0.625 (3)	0.946 (2)	4 (1)*
C(6)	0.974 (3)	0.477 (3)	0.931 (2)	4 (1)*
C(7)	0.496 (3)	0.906 (3)	0.940 (2)	5 (1)*
C(8)	0.420 (2)	0.757 (4)	0.935 (2)	7 (2)*

[a] For the atoms depicted in Figure 5. A complete set of positional parameters is available in the supplementary material. Values marked with an asterisk indicate that the associated atoms were refined isotropically. Anisotropically refined atoms are given in the form of the isotropic equivalent thermal parameter defined as $^4/_3[a^2\beta_{11} + b^2\beta_{22} + c^2\beta_{33} + ab(\cos\gamma)\beta_{12} + ac(\cos\beta)\beta_{13} + bc(\cos\alpha)\beta_{23}]$.

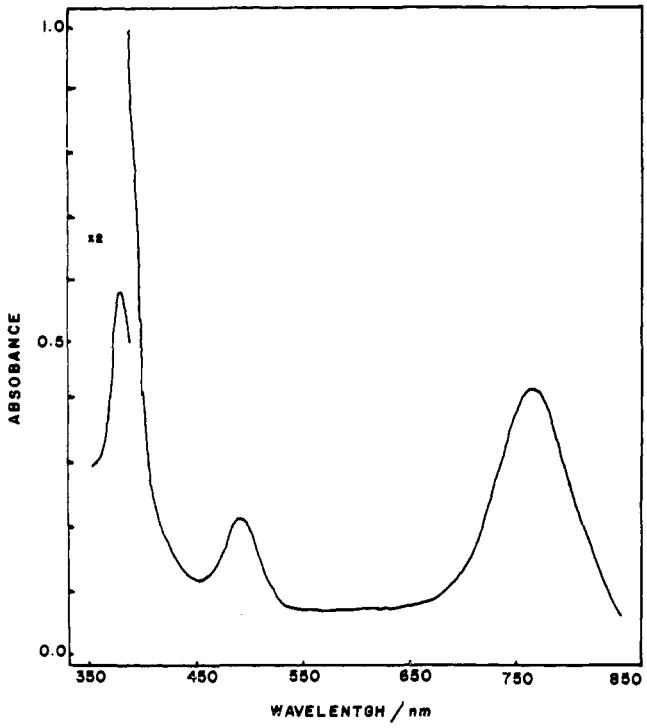

Figure 7. Electronic absorption spectrum of β-$Mo_2Br_4(S,S\text{-dppb})_2$ in THF solution (C = 0.03 mM, l = 1 cm).

than 45° and the $+Z$ direction when the twist is greater than 45°, thus giving rise to left- and right-handed helical charge distributions, respectively. For the same Λ absolute configuration, therefore, the model predicts that a twisted $Mo_2X_4(PP)_2$ complex will have a negative CD if the P–Mo–Mo–P angle is <45° and a positive CD if the twist angle is >45°. In both Λ-Mo_2Cl_4-$(S,S\text{-dppb})_2$ and Λ-$Mo_2Br_4(S,S\text{-dppb})_2$ the twist angles are less than 45° (23 and 22°, respectively), and so we predict negative

Table IX. Principal Bond Distances and Bond Angles in β-$Mo_2Cl_4(S,S\text{-dppb})_2$·THF

Bond Distances (Å)			
Mo(1)–Mo(2)	2.147 (3)	Mo(2)–Cl(3)	2.397 (7)
–Cl(1)	2.397 (8)	–Cl(4)	2.402 (8)
–Cl(2)	2.404 (8)	–P(2)	2.556 (8)
–P(1)	2.568 (8)	–P(4)	2.572 (8)
–P(3)	2.569 (8)		
Bond Angles (deg)			
Mo(2)–Mo(1)–Cl(1)	106.2 (2)	Mo(1)–Mo(2)–Cl(3)	105.2 (2)
–Cl(2)	107.9 (2)	–Cl(4)	107.2 (2)
–P(1)	103.5 (2)	–P(2)	104.2 (2)
–P(3)	105.8 (2)	–P(4)	101.7 (2)
Cl(1)–Mo(1)–Cl(2)	145.8 (3)	Cl(3)–Mo(2)–Cl(4)	144.4 (3)
–P(1)	86.0 (3)	–P(2)	84.7 (8)
–P(3)	82.1 (3)	–P(4)	90.2 (3)
Cl(2)–Mo(1)–P(1)	89.0 (3)	Cl(4)–Mo(2)–P(2)	83.6 (3)
–P(3)	85.9 (3)	–P(4)	85.8 (3)
P(1)–Mo(1)–P(3)	150.4 (3)	P(2)–Mo(2)–P(4)	153.9 (3)

Table X. Principal Bond Distances and Bond Angles in β-$Mo_2Cl_4(S,S\text{-dppb})_2$·$4CH_3CN$

Bond Distances (Å)			
Mo(1)–Mo(2)	2.144 (2)	Mo(2)–Cl(21)	2.398 (4)
–Cl(11)	2.400 (3)	–Cl(22)	2.406 (3)
–Cl(12)	2.397 (3)	–P(21)	2.571 (3)
–P(11)	2.575 (3)	–P(22)	2.550 (3)
–P(12)	2.582 (3)		
Bond Angles (deg)			
Mo(2)–Mo(1)–Cl(11)	106.6 (1)	Mo(1)–Mo(2)–Cl(21)	107.8 (1)
–Cl(12)	108.5 (1)	–Cl(22)	106.6 (1)
–P(11)	103.9 (1)	–P(21)	103.9 (1)
–P(12)	103.0 (1)	–P(22)	104.8 (1)
Cl(11)–Mo(1)–Cl(12)	144.8 (1)	Cl(21)–Mo(2)–Cl(22)	145.5 (2)
–P(11)	84.9 (1)	–P(21)	87.8 (1)
–P(12)	87.2 (1)	–P(22)	84.2 (2)
Cl(12)–Mo(1)–P(11)	84.9 (1)	Cl(22)–Mo(2)–P(21)	87.8 (1)
–P(12)	88.0 (1)	–P(22)	85.1 (2)
P(11)–Mo(1)–P(12)	153.2 (1)	P(21)–Mo(2)–P(22)	151.3 (1)

Table XI. Principal Bond Distances and Angles in β-$Mo_2Br_4(S,S\text{-dppb})_2$

Bond Distances (Å)			
Mo(1)–Mo(2)	2.147 (6)	Mo(3)–Mo(4)	2.152 (6)
–Br(1)	2.535 (7)	–Br(5)	2.548 (7)
–Br(2)	2.533 (8)	–Br(6)	2.529 (7)
–P(1)	2.591 (13)	–P(5)	2.567 (15)
–P(3)	2.603 (14)	–P(7)	2.612 (14)
Mo(2)–Br(3)	2.542	Mo(4)–Br(7)	2.527 (7)
–Br(4)	2.542 (7)	–Br(8)	2.538 (7)
–P(2)	2.587 (15)	–P(6)	2.617 (15)
–P(4)	2.595 (14)	–P(8)	2.575 (15)
Bond Angles (deg)			
Mo(2)–Mo(1)–Br(1)	109.2 (3)	Mo(4)–Mo(3)–Br(5)	108.9 (3)
–Br(2)	109.4 (3)	–Br(6)	108.7 (2)
–P(1)	103.3 (3)	–P(5)	103.9 (4)
–P(3)	104.4 (4)	–P(7)	104.4 (4)
Br(1)–Mo(1)–Br(2)	141.4 (2)	Br(5)–Mo(3)–Br(6)	142.4 (3)
–P(1)	84.3 (3)	–P(5)	84.9 (4)
–P(3)	85.6 (3)	–P(7)	85.3 (3)
Br(2)–Mo(1)–P(1)	87.6 (4)	Br(6)–Mo(3)–P(5)	86.9 (4)
–P(3)	84.5 (4)	–P(7)	85.3 (3)
P(1)–Mo(1)–P(3)	152.3 (4)	P(5)–Mo(3)–P(7)	151.7 (4)
Mo(1)–Mo(2)–Br(3)	108.4 (3)	Mo(3)–Mo(4)–Br(7)	109.1 (3)
–Br(4)	108.0 (3)	–Br(8)	108.3 (3)
–P(2)	105.5 (4)	–P(6)	104.2 (4)
–P(4)	103.8 (4)	–P(8)	103.7 (4)
Br(3)–Mo(2)–Br(4)	143.6 (8)	Br(7)–Mo(4)–Br(8)	142.6 (3)
–P(2)	84.9 (4)	–P(6)	85.1 (4)
–P(4)	85.2 (4)	–P(8)	85.5 (4)
Br(4)–Mo(2)–P(2)	84.6 (4)	Br(8)–Mo(4)–P(6)	85.0 (4)
–P(4)	87.1 (3)	–P(8)	86.6 (4)
P(2)–Mo(2)–P(4)	150.7 (5)	P(6)–Mo(4)–P(8)	152.1 (5)

Table XII. Circular Dichroism Spectra of β-$Mo_2X_4(S,S\text{-dppb})_2$, X = Cl, Br

obsd band position, cm^{-1}						predicted sign			
						$\delta\Lambda\delta$		$\delta\Delta\delta$	
β-Mo_2Cl_4-$(S,S\text{-dppb})_2$	$\Delta\epsilon$	β-Mo_2Br_4-$(S,S\text{-dppb})_2$	$\Delta\epsilon$	sign	assignt	$\phi < 45°$	$\phi > 45°$	$\phi < 45°$	$\phi > 45°$
13 513	7.6	13 158	6.4	−	$\delta_{xy} \rightarrow \delta^*_{xy}$ B_1	−	+	+	−
17 241	1.3	17 094	2.8	−	$\delta_{xy}^2 \rightarrow \delta^{*2}_{xy}$ A	−	+	+	−
21 277	48	20 408	51.2	+	$\delta_{xy} \rightarrow \delta_{x^2-y^2}$ B_1	+	−	−	+
23 810	13	23 256	12	+	$\delta_{xy} \rightarrow \delta^*_{x^2-y^2}$ A	+	−	−	+
27 027	11.2	26 316	20.8	+	$\pi_{yz} \rightarrow \delta^*_{xy}$ B_2	+	−	−	+
29 851	16	30 303	9.6	+	$\pi_{xz} \rightarrow \delta^*_{xy}$ B_1	+	−	−	+
32 895	17.6	31 746	24	−	$\pi_{yz} \rightarrow \delta_{x^2-y^2}$ B_2	−	+	+	−

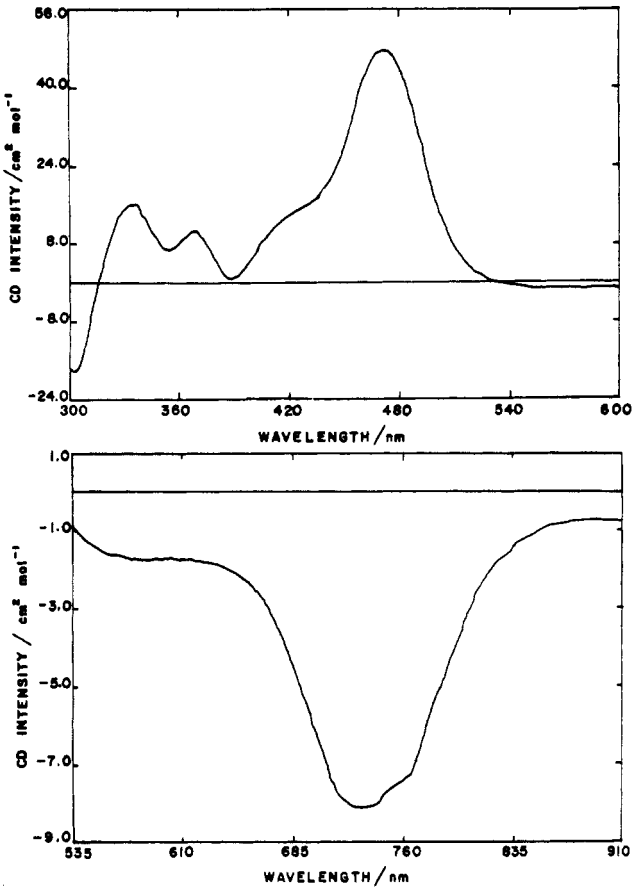

Figure 8. Circular dichroism spectrum of β-$Mo_2Cl_4(S,S\text{-dppb})_2$ in THF solution.

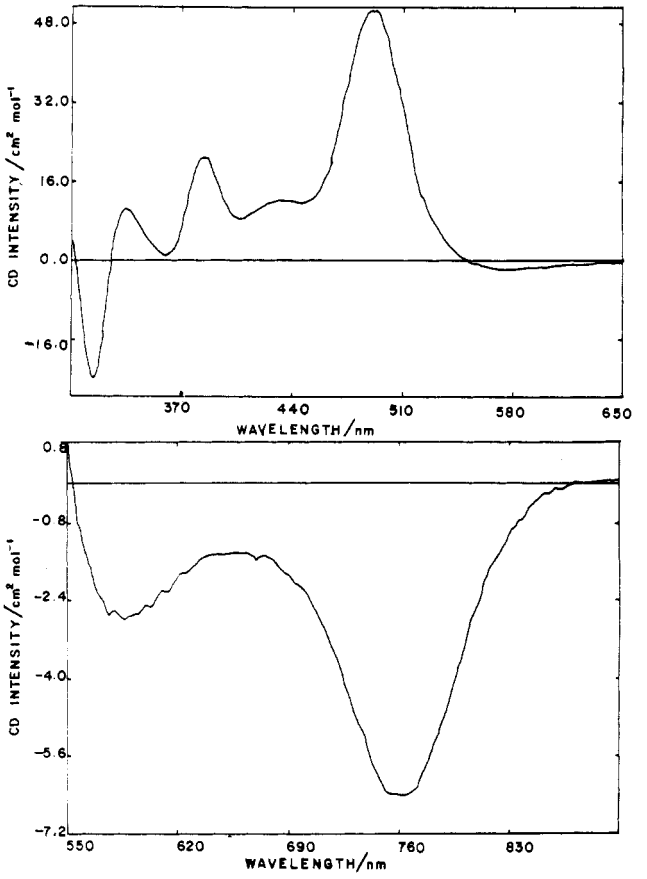

Figure 9. Circular dichroism spectrum of β-$Mo_2Br_4(S,S\text{-dppb})_2$ in THF solution.

CD for the $\delta_{xy} \rightarrow \delta^*_{xy}$ transition, as is experimentally observed.

CD of the $\delta_{xy} \rightarrow \delta_{x^2-y^2}$ Transition. Perhaps the most noticeable feature in the spectra of Λ-$Mo_2Cl_4(S,S\text{-dppb})_2$ and Λ-$Mo_2Br_4(S,S\text{-dppb})_2$ is the transition in the middle of the spectrum (470 nm in the chloride and 490 nm in the bromide complex). Although the absorptions are much weaker than those of the corresponding $\delta_{xy} \rightarrow \delta^*_{xy}$ transitions, the associated CD bands are between 6 and 8 times stronger, making the dissymmetry factor (the ratio $\Delta\epsilon/\epsilon$) approximately 1 order of magnitude larger for this transition than for the $\delta_{xy} \rightarrow \delta^*_{xy}$ transition. Dissymmetry factors of this magnitude are usually indicative[15] of magnetic-dipole-allowed, electric-dipole-forbidden transitions in the parent achiral chromophore. The only plausible assignments are $\delta_{xy} \rightarrow \delta_{x^2-y^2}$ and $\pi_{xz,yz} \rightarrow \delta^*_{xy}$, of which the former is calculated to occur at lower energy. If we assign the transition in the 470–490-nm region to $\delta_{xy} \rightarrow \delta_{x^2-y^2}$, we may relate the sign of the CD to the twist angle of the $Mo_2X_4P_4$ chromophore in a manner exactly analogous to that used for the $\delta_{xy} \rightarrow \delta^*_{xy}$ transition, as is shown in Figure 11. The Λ absolute configuration is once again illustrated, and a consideration of the transient charge distributions shows that a twist of less than 45° will produce a right-handed helical charge displacement and so a positive CD while a twist of greater than 45° will produce a left-handed helical displacement and so a negative CD. Once again, our prediction agrees with experiment for the two complexes we have structurally characterized.

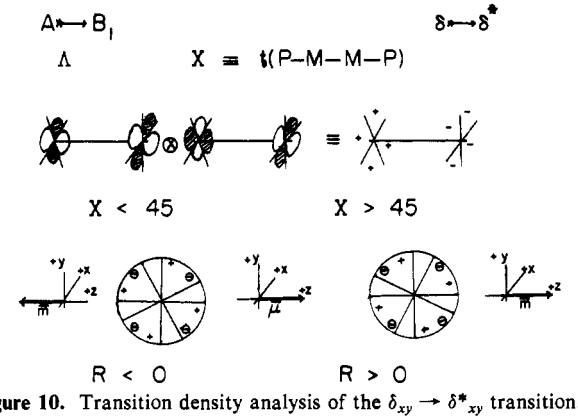

Figure 10. Transition density analysis of the $\delta_{xy} \rightarrow \delta^*_{xy}$ transition.

Assignment of the Remaining Transitions. The assignment of the remaining transitions along with their predicted CD signs and experimental signs and magnitudes are given in Table XII. The high-energy shoulder seen on the CD band associated with $\delta_{xy} \rightarrow \delta_{x^2-y^2}$ is assigned to the "companion" $\delta_{xy} \rightarrow \delta^*_{x^2-y^2}$ transition while

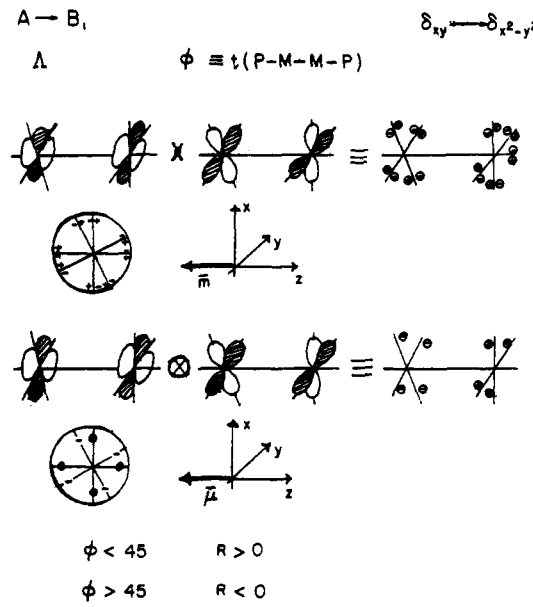

Figure 11. Transition density analysis of the $\delta_{xy} \rightarrow \delta_{x^2-y^2}$ transition.

the next two CD bands are believed to be due to the magnetic dipole $\pi_{yz} \rightarrow \delta^*_{xy}$ and $\pi_{xz} \rightarrow \delta^*_{xy}$ transitions. The highest energy CD is assigned as the electron-dipole-allowed $\pi_{yz} \rightarrow \delta_{x^2-y^2}$ transition. A weak but real CD is observed in the gap between the $\delta_{xy} \rightarrow \delta^*_{xy}$ and $\delta_{xy} \rightarrow \delta_{x^2-y^2}$ transitions, and on careful examination, weak absorption can be detected also. There is no obvious one-electron transition that could give rise to such a very weak absorption (much weaker than the $\delta_{xy} \rightarrow \delta_{x^2-y^2}$ magnetic-dipole transition) in this energy region. We therefore assign the transition as the magnetic- and electric-dipole-forbidden two-electron promotion $\delta_{xy}^2 \rightarrow \delta^{*2}_{xy}$. The energy of this transition is much less than twice its one-electron counterpart, but this is not unexpected since it is known that the electron correlation energy is a major contributor to the $\delta_{xy} \rightarrow \delta^*_{xy}$ energy.

Acknowledgment. We thank the National Science Foundation for support of the work at Texas A&M University, and the SERC for a studentship (to I.F.F.).

Registry No. β-$Mo_2Cl_4(S,S\text{-dppb})_2 \cdot C_4H_8O$, 88968-77-8; β-$Mo_2Cl_4(S,S\text{-dppb})_2 \cdot 4CH_3CN$, 89015-84-9; β-$Mo_2Br_4(S,S\text{-dppb})_2 \cdot {}^1/_2C_4H_8O$, 102341-14-0; $Mo_2(O_2CCF_3)_4$, 36608-07-8; $K_4Mo_2Cl_8$, 25448-39-9; Mo, 7439-98-7.

Supplementary Material Available: A table of anisotropic thermal displacement parameters and a view of the entire molecule of β-$Mo_2Cl_4(S,S\text{-dppb})_2$ showing the atom-labeling scheme used in the crystal structure of the THF solvate (Figure 2), a complete table of positional parameters for β-$Mo_2Br_4(S,S\text{-dppb})_2$, listings of general temperature factors for all three structures, and complete tables of bond lengths and angles for all three structures (27 pages). Ordering information is given on any current masthead page.

Contribution from the Department of Chemistry,
University of Minnesota, Minneapolis, Minnesota 55455

Synthesis and Reactivity of $[(\eta^5\text{-}C_5R_5)Ru(\eta^6\text{-arene})]PF_6$ (R = H, CH_3) Complexes of Naphthalene, Anthracene, Pyrene, Chrysene, and Azulene. Kinetic Studies of Arene Displacement Reactions in Acetonitrile Solutions

Amy M. McNair and Kent R. Mann*

Received November 4, 1985

The synthesis and characterization of new $[(\eta^5\text{-}C_5H_5)Ru(\eta^6\text{-arene})]PF_6$ and $[(\eta^5\text{-}C_5(CH_3)_5)Ru(\eta^6\text{-arene})]PF_6$ complexes are reported (arene = naphthalene, anthracene, pyrene, chrysene, azulene). Kinetic studies of arene displacement by acetonitrile for five of these complexes are reported. The values obtained for k_{obsd} range from 1.3×10^{-2} s^{-1} to 4.6×10^{-6} s^{-1} in 2.73 M CH_3CN. The differences between the rates observed for the $C_5H_5^-$ complexes and the $C_5(CH_3)_5^-$ compound are explained in terms of an associative mechanism. Rate constants for the ruthenium compounds containing pyrene and chrysene were found to be approximately 4 orders of magnitude larger, respectively, than those for the corresponding Fe complexes. This is believed to be an effect of the difference in the sizes of the two metals and their subsequent susceptibility toward nucleophilic attack. The temperature and concentration dependence of the rate constant k was studied for the reaction of $[(\eta^5\text{-}C_5(CH_3)_5)Ru(\eta^6\text{-anthracene})]^+$ with CH_3CN. The ΔS^* of −13.3 (9) eu and ΔH^* = +14.9 (3) kcal/mol confirm the associative nature of the displacement reaction. The straight-line plot obtained for k_{obsd} vs. $[CH_3CN]$ is consistent with a rate equation of the general form rate = $k[M][CH_3CN]$ where [M] is the concentration of the metal complex. Two mechanisms consistent with the data are proposed and discussed; one includes a preequilibrium between a η^6-arene metal complex and a η^4-arene species, while the other involves direct nucleophilic attack on the metal center of the η^6 complex.

Introduction

Work in our group has concentrated on the photochemical replacement of arenes in $[(\eta^5\text{-}C_5H_5)M(\eta^6\text{-arene})]^+$ and $[(C^5\text{-}C_5(CH_3)_5)M(\eta^6\text{-arene})]^+$ complexes (M = Fe, Ru; $C_6H_5^-$ = cyclopentadienyl anion, $C_5(CH_3)_5^-$ = pentamethylcyclopentadienyl anion; arene = substituted benzene) with ligands such as acetonitrile.[1-4] The photochemical ring-release mechanism is dependent on the nucleophilicity of the incoming ligand and the electronic and steric characteristics of the arene ring. Acetonitrile attack at the metal-centered excited state is believed to be the primary step in these reactions. For arene = substituted benzene, the thermal replacement of the arene by three acetonitrile ligands has not been observed. We now wish to report the synthesis and reactivity of polycyclic aromatic $[(\eta^5\text{-}C_5H_5)Ru(\eta^6\text{-arene})]^+$ and $[(\eta^5\text{-}C_5(CH_3)_5)Ru(\eta^6\text{-arene})]^+$ complexes with the arenes naphthalene, anthracene, pyrene, and chrysene and the pseudo-arene azulene. Many of these new compounds exhibit facile *thermal*

* To whom correspondence should be addressed.

(1) Gill, T. P.; Mann, K. R. *Organometallics* **1982**, *1*, 485.
(2) Schrenk, J. L.; Palazzotto, M. C.; Mann, K. R. *Inorg. Chem.* **1983**, *22*, 4047.
(3) McNair, A. M.; Schrenk, J. L.; Mann, K. R. *Inorg. Chem.* **1984**, *23*, 2633.
(4) Gill, T. P.; Mann, K. R. *Inorg. Chem.* **1980**, *19*, 3007.

0020-1669/86/1325-2519$01.50/0